Molecular Pharmacology Fast Forward. Published on June 13, 2012 as doi:10.1124/mol.112.079715
This article has not been copyedited and formatted. The final version may differ from this version.

Common mechanisms of drug interactions with sodium and T-type calcium channels

Chris Bladen and Gerald W. Zamponi

Department of Physiology & Pharmacology, Hotchkiss Brain Institute, University of Calgary, Canada.

Molecular Pharmacology Fast Forward. Published on June 13, 2012 as DOI: 10.1124/mol.112.079715
This article has not been copyedited and formatted. The final version may differ from this version.

Running title: Mixed Nav/Cav3 blockers

Address for correspondence: Gerald W. Zamponi Ph.D., FRSC. Department of Physiology and Pharmacology, University of Calgary, 3330 Hospital Dr. NW, Calgary, AB, T2N 4N1, Canada. Tel. (403) 220-8687. Email: Zamponi@ucalgary.ca

Number of text pages: 26

Number of tables: 2

Number of figures: 8

Number of references: 36

Number of words in Abstract: 210

Number of words in Introduction: 508

Number of words in Discussion: 412

List of non-standard abbreviations: A803467 [5-(4-chlorophenyl-N-(3,5-dimethoxyphenyl)furan-2-carboxamide], TTX tetrodotoxin

Molecular Pharmacology Fast Forward. Published on June 13, 2012 as DOI: 10.1124/mol.112.079715
This article has not been copyedited and formatted. The final version may differ from this version.

Abstract:

Voltage-gated sodium (Nav) and calcium (Cav) channels play important roles in physiological processes, including neuronal and cardiac pacemaker activity, vascular smooth muscle contraction and nociception. They are thought to share a common ancestry and in particular, T-type calcium channels (T-type) share structural similarities with Nav channels, both with regard to membrane topology and with regard to gating kinetics, including rapid inactivation. We thus reasoned that certain drugs acting on Nav channels may also modulate the activities of T-type channels. Here we show that the specific Nav1.8 blocker A803467 tonically blocks T-type channels in the low micromolar range. Similarly to Nav1.8, this compound causes a significant hyperpolarizing shift in the voltage dependence of inactivation and appears to promote a slow inactivation-like phenotype. We further hypothesized that the structural similarity between T-type and Nav channels may extend to structurally similar drug binding sites. Sequence alignment revealed several highly conserved regions between T-type and Nav channels that corresponded to drug binding sites known to alter voltage-dependent gating kinetics. Mutation of amino acid residues in this regions within human Cav3.2 T-type channels altered A803467 blocking affinity several-fold, suggesting that these sites may be exploited for the design of mixed T-type and Nav channel blockers that could potentially act synergistically to normalize aberrant neuronal activity.

Molecular Pharmacology Fast Forward. Published on June 13, 2012 as DOI: 10.1124/mol.112.079715
This article has not been copyedited and formatted. The final version may differ from this version.

Introduction:

Nav channels mediate the induction and propagation of action potentials in most electrically excitable cells (Yu and Catterall, 2004). The mammalian genome encodes nine different types of Nav α subunits that are functionally classified as either tetrodotoxin-sensitive (TTX-S) or tetrodotoxin-resistant (TTX-R), with the latter exhibiting slower inactivation kinetics than other Nav channel subtypes (Waxmann et al., 1999; Blair and Bean, 2002). The various Nav channel α subunits share a common transmembrane topology of four homologous domains that each contain six membrane spanning helices plus a p-loop. While the α subunits define the Nav channel isoform and contain all of the machinery to form a sodium selective voltage activated channel, their functional properties are modulated by association with ancillary β1 and β2 subunits (for review see Isom, 2001). Mutations in various Nav channel subunits have been linked to disorders such as paramyotonia congenita, cardiac arrhythmias, epilepsy and both hypersensitivity and insensitivity to pain, thus underscoring their importance for nerve, muscle and heart function (Catterall et al., 2008; Jarecki et al., 2010).

Low-voltage-activated (LVA) i.e., T-type channels, trigger low-threshold depolarizations that in turn lead to the initiation of action potentials (Bender et al., 2011; Cain and Snutch, 2010). These channels can be activated by small membrane depolarizations and display a small single channel conductance and compared to other Cav channel subtypes, they display rapid activation and inactivation kinetics (Perez-Reyes, 2003). T-type channels are encoded by one of three different types of Cav3 α1 subunits (Cav3.1, Cav3.2 and Cav3.3) whose membrane topology is similar to that of Nav channels (Catterall et al., 2005). Mutations in Cav3.2 T-type channels have been linked to absence seizures (Heron et al., 2007; Khosravani and Zamponi, 2006). Moreover, upregulation of Cav3.2 T-type channel activity in primary afferent fibers has been linked to the

development of chronic pain (for review see Altier and Zamponi, 2004; Park and Luo, 2010) and T-type channel dysfunction contributes to cardiac hypertrophy (Cribbs, 2010; David et al., 2010). Altogether, Nav channels and T-type channels both contribute to neuronal excitability and to similar disorders such as epilepsy and pain. Indeed, knockout of Nav1.8 and Cav3.2 both result in hyposensitivity to pain (see Wang et al., 2011; Cregg et al., 2010 for reviews), suggesting the possibility that mixed Nav/T-type channel blockers may be a possible strategy for the development of new analgesics (Hildebrand et al., 2010). Recently, a new inhibitor of Nav1.8 channels, A803467, has been shown to be efficacious in animal pain models (McGaraughty et al., 2008). The interaction site of A803467 on the Nav channel complex is unknown, but its mode of action appears to be preferential binding to the slow inactivated state of this channel (Jarvis et al., 2007).

Here we show that A803467 inhibits T-type channels in the low micromolar range and mediates a hyperpolarizing shift in the voltage dependence of activation and inactivation. In addition, the compound promotes a slow inactivation-like phenotype. Sequence alignment between T-type and Nav channels and their local anesthetic interaction site identified key residues involved in the blocking action of this compound on T-type channels.

Molecular Pharmacology Fast Forward. Published on June 13, 2012 as DOI: 10.1124/mol.112.079715
This article has not been copyedited and formatted. The final version may differ from this version.

Materials and Methods:

CDNA Constructs. Human Cav3.2, rat Cav1.2, and rat Cav2.1 cDNA constructs, as well as ancillary Cav channel subunit cDNAs were kindly provided by Dr. Terrance Snutch (University of British Columbia, Vancouver, Canada). Human Cav3.3 was obtained from Dr. Arnaud Monteil (CNRS, Montpelllier, France), and human Cav3.1 was described previously by our laboratory (Beedle et al., 2002).

Site-Directed Mutagenesis. Site-Directed Mutagenesis was performed using the QuikChange II™ Site-Directed Mutagenesis Kit and protocols from Agilent Technologies Inc. Mutations were then verified by on-site sequencing of the full length cDNA clone.

Chemicals. Unless stated otherwise, chemicals were purchased from Sigma (St. Louis, MO). A803467 was purchased from Tocris Bioscience (Ellisville, MO) and was dissolved in dimethyl sulfoxide (DMSO) at the stock concentrations of 10 mM or 30 mM. Dilutions were made in external recording solutions so that the final concentration of DMSO was 0.1% or less. Cav channel currents were not affected by 0.1% DMSO.

tsA-201 Cell Culture and Transfection. Human embryonic kidney tsA-201 cells were cultured and transfected using the calcium phosphate method as described previously (Altier et al., 2006). Enhanced green fluorescent protein (EGFP) DNA (0.5 µg of EGFP; Clontech) was transfected as a marker. For experiments involving L- and P/Q type channels, rCav1.2 or rCav2.1, α1 subunits (3 µg), were each co-transfected with rat β1b (3 µg) or rat β4 (3 µg). For experiments involving T-type channels, hCav3.1, hCav3.2, and hCav3.3, α1subunits were transfected alone (6 µg).

Molecular Pharmacology Fast Forward. Published on June 13, 2012 as DOI: 10.1124/mol.112.079715
This article has not been copyedited and formatted. The final version may differ from this version.

Cells were resuspended with 0.25% (w/v) trypsin-EDTA (Invitrogen) and plated on glass cover slips a minimum of 3 to 4 hours before patching and kept at 37°C and 5% CO2.

Electrophysiology. Whole-cell voltage-clamp recordings on tsA- 201 cells were performed at room temperature 2 to 3 days after transfection. The external recording solution for calcium channel recordings contained (in mM): 142 CsCl, 2 $CaCl_2$, 1 $MgCl_2$, 10 HEPES, 10 Glucose, adjusted to pH 7.4 with CsOH. The external recording solution for hCav3.2 Q1848 mutations and their hCav3.2 wild type controls contained 124 Cscl, 20 $BaCl_2$, 1 $MgCl_2$, 10 HEPES, 10 Glucose, adjusted to pH 7.4 with CsOH. For all recordings, the internal patch pipette solution contained (in mM): 126.5 $CsMeSO_4$, 2 $MgCl_2$, 11 EGTA, 10 HEPES adjusted to pH 7.3 with CsOH. The internal solution was supplemented with 0.6 mM GTP and 2 mM ATP, which were added directly to the internal solution immediately before use. Liquid junction potentials for the above solutions were left uncorrected.

Drugs were prepared daily in external solution and were applied locally to cells with the use of a custom built gravity driven microperfusion system that allows solution exchanges in approximately 1 second (Feng et al., 2003). A series of vehicle only control experiments was performed to ensure that there were no time dependent shifts in half-activation and half-inactivation potentials, and no such changes were observed (data not shown). Currents were elicited from a holding potential of -110 mV and were measured by conventional whole-cell patch clamp using an Axopatch 200B amplifier in combination with Clampex 9.2 software (Molecular Devices, Sunnyvale, CA). After establishment of the whole cell configuration, cellular capacitance was minimized using the analog compensation available on the amplifier. Series resistance was <10 MΩ and was compensated >85% in all experiments. Data were filtered

Molecular Pharmacology Fast Forward. Published on June 13, 2012 as DOI: 10.1124/mol.112.079715
This article has not been copyedited and formatted. The final version may differ from this version.

at 1 kHz (8-pole Bessel) and digitized at 10 kHz with a Digidata 1320 interface (Molecular Devices). In addition to collecting the raw data, a p/4 online leak-subtraction protocol was used (the p/4 protocol involved four very brief hyperpolarizing pulses which should have a negligible effect on drug interactions). Non leak subtracted currents were acquired in parallel for quality control purposes. For current-voltage relation studies, the membrane potential was held at -110 mV and cells were depolarized from -90 to 20 mV in 10 mV increments. For steady-state inactivation studies, the membrane potential was depolarized by test pulses to -30 mV after 3.6-s conditioning prepulses ranging from -110 to -20 mV. Individual sweeps were separated by 10 seconds to allow for complete recovery from inactivation between conditioning pulses. The current amplitude obtained from each test pulse was then normalized to that observed at a holding potential of -110 mV. For slow inactivation studies channels were assessed using a test pulse (P2) that followed a 10-s conditioning prepulse of between -70 or -80mV to elicit a peak current amplitude that was approximately 50 to 60% of the initial test pulse (P1).

Data Analysis and Statistics. Data were analyzed using Clampfit 9.2 (Molecular Devices). Preparation of figures and curve fitting was carried out with Origin 7.5 software (Northampton, MA, USA). Current-voltage relationships were fitted with the modified Boltzmann equation: $I = [G_{max}*(V_m-E_{rev})]/[1+\exp[(V_{0.5act}-V_m)/k_a]$, where V_m is the test potential, $V_{0.5act}$ is the half-activation potential, E_{rev} is the reversal potential, G_{max} is the maximum slope conductance, and k_a reflects the slope of the activation curve. Data from concentration-dependence studies were fitted with the equation $y = A2 + (A1-A2)/(1 + ([C]/IC_{50})^n)$ where A_1 is initial current amplitude and A_2 is the current amplitude at saturating drug concentrations, [C] is the drug concentration and n is the Hill coefficient. Statistical significance was determined by paired or unpaired Student's *t*-

Molecular Pharmacology Fast Forward. Published on June 13, 2012 as DOI: 10.1124/mol.112.079715
This article has not been copyedited and formatted. The final version may differ from this version.

Tests and one-way or repeated measures ANOVA followed by Tukey's Multiple Comparison tests and significant values were set as indicated in the text and figure legends. All data are given as means +/- standard errors. Steady-state inactivation curves were fitted using the Boltzmann equation: $I = 1/(1 + \exp[(V_m - V_h)/S]$ where V_h is the half-inactivation potential and S is the slope factor.

Molecular Pharmacology Fast Forward. Published on June 13, 2012 as DOI: 10.1124/mol.112.079715
This article has not been copyedited and formatted. The final version may differ from this version.

Results:

A803467 blocks T-type channels

A recent study identified a novel compound (A803467) as a specific and potent blocker of TTX-R hNav1.8 channels (Jarvis et al., 2007). Given that T-type channels share structural similarities with Nav channels, we examined whether this compound may affect T-type channels at both therapeutic plasma and brain tissue concentrations (10 to 17 μM and 3 to 5 μM, respectively, Jarvis et al., 2007). Figures 1A and 1B illustrate the effect of 5 μM A803467 on human Cav3.2 channels expressed transiently in tsA-201 cells at a holding potential of -110 mV. As evident from the figure, this compound mediated robust peak current inhibition that could be partially reversed upon washout. The concentration dependence of this type of tonic (i.e., resting state) block could be well described by a Hill coefficient close to 1 (Figure 1C), suggesting a bimolecular interaction between the channel and the blocker. We then examined the calcium channel subtype selectivity of A803467 (Figure 1D) and found that all LVA sub-types were blocked with IC50s in the low micromolar range, whereas two representative members of the high voltage activated (HVA) channel family (i.e., L- and P/Q type channels) exhibited lower affinities (i.e., higher IC50 values). A previous study has shown that this drug does not show significant block of N-type calcium channels, TRPV1, KCNQ2/3 potassium channels and other channels or receptors found in peripheral sensory neurons (Jarvis et al., 2007).

Unlike what has been reported for hNav1.8 channels (Jarvis et al., 2007), we observed a significant hyperpolarizing shift in the half-activation voltages of both Cav3.1 and Cav3.2 channels (Figure 2). There was also a trend towards more hyperpolarized voltages for hCav3.3, however, these did not reach statistical significance (see Table 1). Application of A803467 to T-type channels also resulted in a significant (~10mV) hyperpolarizing shift in the half-inactivation

Molecular Pharmacology Fast Forward. Published on June 13, 2012 as DOI: 10.1124/mol.112.079715
This article has not been copyedited and formatted. The final version may differ from this version.

potentials of hCav3.1 and hCav3.2 (see Figure 2C, 2D) similar to that described previously for hNav1.8 channels (Jarvis et al., 2007). The leftward shift in the steady state inactivation curve is consistent with inactivated channel block (Hille, 1977).

Altogether, these data indicate that A803467 mediates both resting channel inhibition and inactivated channel block of T-type channels.

A803467 block promotes a slow inactivation-like state of hCav3.2

Previous studies have identified slow inactivation channel blockers of Navs (Sheets et al., 2008), as well as mixed sodium/T-type channel blockers which stabilize the slow inactivated conformation of these channels (Hildebrand et al., 2010). To determine whether A803467 may mediate a similar action on T-type channels, we used a slow inactivation protocol to induce a partial slow inactivated-like state of the channel. Specifically, we applied a brief test depolarization (P1) prior to a 10 s conditioning pulse to -70 mV which is expected to induce both fast and slow inactivation. This was followed by a brief hyperpolarizing step to induce recovery from fast inactivation of non drug-bound channels. A second depolarizing test pulse (P2) allowed us to determine the fraction of channels in the slow inactivated-like state (under our experimental conditions, this amounted to about 30% slow inactivation in the absence of the drug). The dose-dependent effects of A803467 on the currents elicited by P1 and P2 were then compared to ascertain the amount of resting vs. slow inactivated-like channel block. As shown in Figure 3, hCav3.2 channels A803467 induced channel inhibition that resembled features of enhanced slow inactivation, as evident from a reduction in the IC50 of P2 current inhibition. In contrast, the hCav3.1 and hCav3.3 channels did not show stabilization of the slow inactivated-like channel conformation. The combined effects of A8023467 on different kinetic states of hCav3.2 channels

Molecular Pharmacology Fast Forward. Published on June 13, 2012 as DOI: 10.1124/mol.112.079715
This article has not been copyedited and formatted. The final version may differ from this version.

predicts substantial total/combined inhibition of Cav3.2 currents in the high nanomolar to the low micromolar range which is well within the therapeutic range of A803467.

A locus analogous to the Nav local anesthetic binding site controls A803467 block of Cav3.2

Given the structural similarity between T-type and Nav channels, we hypothesized that the drug binding site on these two types of channels may be conserved. Sodium channels possess multiple drug interaction sites, including a receptor site for binding of local anesthetics and anticonvulsive drugs (Lipkind and Fozzard, 2005). A key locus for local anesthetic block of Nav channels was first identified by Ragsdale and colleagues (1994). The authors revealed that tyrosine (Tyr) 1771 and phenylalanine (Phe) 1764 in Nav1.2 were important determinants of local anesthetic block of Nav1.2 channels and that mutagenesis of these two residues (especially reside 1764) resulted in a reduction in etidocaine blocking affinity for the channel. In hCav3.2 channels, the residue equivalent to these two residues are valine and glutamine (Figure 4) indicating that one key component of the local anesthetic binding site is absent in T-type channels. However, Yarov-Yarovoy and colleagues (2001, 2002) identified several amino acid residues in the IS6 and III S6 segments of the Nav 1.2 α subunit that also affected drug interactions. These authors showed that in addition to residue Tyr 1771 and Phe 1764, mutagenesis of isoleucines (Ile) 409 and 1469 reduced local anesthetic interactions. ClustalW2 multiple sequence alignment of hNav1.8 versus hNav1.2 and hCav 3.2 revealed that these regions were highly conserved in these channels (see Figure 4). The corresponding loci of these residues in Cav3.2 are Ile 403 and Val 1551, indicating that Cav3.2 channels may possess some of the structures needed for local anesthetic interactions.

Molecular Pharmacology Fast Forward. Published on June 13, 2012 as DOI: 10.1124/mol.112.079715
This article has not been copyedited and formatted. The final version may differ from this version.

To determine whether these residues may be involved in A803467 interactions with hCav3.2, we replaced Ile 403 and Val 1551 with alanines and then assessed A803467 block of these mutant channels. As shown in Figure 5, these amino acid substitutions resulted in a significant decrease in A803467 blocking affinity for hCav3.2 (by over one order of magnitude for the IIIS6 substitution). This effect was not secondarily due to reduced slow inactivation, as the only gating parameter that was significantly altered was a shift in half-activation voltage of the I403A mutant (see Table 2).

Next, we tested whether these mutations affected the ability of A803467 to enhance slow inactivation of hCav3.2. As shown in Figure 6, the A803467-induced stabilization of a slow inactivated like state of the wild type channel was abolished in the two mutant channels.
To further support the hypothesis that a locus analogous to the sodium local anesthetic binding site controls A803467 block of Cav3.2, we introduced a tyrosine residue in position V1855 of Cav3.2 (corresponding to Tyr 1771 in hNav1.2) and determined the consequences on A803467 block of hCav3.2 (Figure 7). The introduction of Tyr 1855 significantly increased A803467 resting state blocking affinity by approximately four-fold (Figure 7A) and preserved the ability of the compound to stabilize the fast inactivated state (Figure 7B). Furthermore, we observed a significant increase in blocking activity in response to the slow inactivation pulse paradigm, as evident from a reduction in the IC50 during P2 (Figure 7C). Unlike substitutions in positions 403 and 1551, tyrosine substitution of residue 1855 induced a ~10 mV depolarizing shift in the voltage dependences of activation (not shown) and inactivation (Figure 7B), indicating that this locus is important for channel gating.

Finally, we mutated the glutamine residue in position 1848 of hCav3.2 to the phenylalanine found in the corresponding position in Nav1.2 channels (Ragsdale et al., 1994; see

Figure 4). In addition we also substituted this residue with another hydrophobic residue leucine. When expressed in tsA-201 cells, both mutants yielded T-type currents, albeit with much reduced whole cell current amplitudes compared to those seen with wild type channels. In fact, reliable current recordings required us to increase the ionic strength of the extracellular recording solution to 20 mM barium. Under these conditions, we were at least able to test the ability of A803467 to mediate tonic (resting) blocking affinity. As shown in Figure 8, the compound exhibited a twenty-fold increase in affinity for the phenylalanine mutant, and a ten-fold increase for the leucine mutant compared with wild type channels bathed in the same barium solution. In both mutants, block was completely reversible upon washout, (not shown).

Altogether, these data indicate that both tonic and slow inactivated-like channel block of Cav3.2 channels by A803467 is mediated by interactions of this compound with residues that are analogous to those comprising the local anesthetic receptor site in Nav channels.

Molecular Pharmacology Fast Forward. Published on June 13, 2012 as DOI: 10.1124/mol.112.079715
This article has not been copyedited and formatted. The final version may differ from this version.

Discussion:

A803467 was originally identified as potent inhibitor of hNav1.8 channels with a mode of action that appears to involve at least in part a stabilization of the slow inactivated state (Jarvis et al, 2007). Furthermore, this compound was shown to reduce neuropathic and inflammatory pain in animal models (McGaraughty et al., 2008). Here, we demonstrate that A803467 also blocks T-type channels with high affinity, with IC50's that fall into the range of therapeutic concentrations and that block of the Cav3.2 channel subtype appears to stabilize slow inactivation. The similarities between Nav1.8 and Cav3.2 channel inhibition by this compound are striking and underscored by the observation that mutations in Cav3.2 in regions corresponding to the local anesthetic interaction site in sodium channels antagonize A803467 action. Altogether, our findings suggest evolutionarily conserved interactions between A803467 and related drugs with Nav and LVA Cav channels.

Both hNav1.8 and T-type Cav3.2 channels are functionally expressed in both nociceptive DRG and lamina I spinal cord neurons (Hildebrand et al., 2010; Ikeda et al., 2003) and are known to regulate their excitability. Hyperfunction of both channel subtypes has been linked to the development of hyperalgesia and allodynia in various animal models of pain (Ikeda et al., Barton et al., 2005 and Cummins et al., 2007). Conversely, knockout or inhibition of T-type or Nav channels mediates analgesia (Bourinet et al., 2005 and Choi et al., 2007).

Given the potent blocking effects of A803467 on Cav3.2 channels, it is possible that the previously reported effects of this compound on AP firing in DRG neurons and the associated analgesia may be at least in part mediated by T-type channel inhibition. Given that Nav and Cav work together to prolong subthreshold depolarizations within lamina I neurons (Prescott et al., 2002; Ikeda et al., 2003 and Hildebrand et al., 2010), a dual action of A803467 may promote a

Molecular Pharmacology Fast Forward. Published on June 13, 2012 as DOI: 10.1124/mol.112.079715
This article has not been copyedited and formatted. The final version may differ from this version.

synergistic inhibition of pain signaling. Slow inactivation is significantly enhanced during prolonged depolarizations or during neuronal burst firing. Promotion of a slow inactivated like state of both channel subtypes may thus mediate frequency dependent inhibition of channel activity and therefore reduce overall neuronal excitability. Reduction in neuronal excitability may make compounds such as A803467 ideally suited towards treatment of neuronal hyperexcitability disorders including pain and may perhaps be extended to conditions such as epilepsy. The apparent conservation in the drug receptor site between Nav and Cav3.2 channels may provide an opportunity for the synthesis of more potent antagonists acting on both of these channel subtypes.

Molecular Pharmacology Fast Forward. Published on June 13, 2012 as DOI: 10.1124/mol.112.079715
This article has not been copyedited and formatted. The final version may differ from this version.

Author contributions:

Participated in research design: Bladen and Zamponi.

Conducted experiments: Bladen.

Contributed new reagents or analytic tools: Bladen.

Performed data analysis: Bladen.

Wrote or contributed to the writing of the manuscript: Bladen and Zamponi.

Molecular Pharmacology Fast Forward. Published on June 13, 2012 as DOI: 10.1124/mol.112.079715
This article has not been copyedited and formatted. The final version may differ from this version.

References

Altier C, Khosravani H, Evans RM, Hameed S, Peloquin JB, Vartian BA, Chen L, Beedle AM, Ferguson SS, Mezghrani A, Dubel SJ, Bourinet E, McRory JE, and Zamponi GW (2006) ORL1 receptor-mediated internalization of N-type calcium channels. *Nat Neurosci* **9:**31–40.

Altier C and Zamponi, GW (2004). Targeting Ca2+ channels to treat pain: T-type versus N-type. *Trends Pharmacol Sci* **25**, 465–470.

Barton ME, Eberle EL, and Shannon HE (2005). The antihyperalgesic effects of the T-type calcium channel blockers ethosuximide, trimethadione, and mibefradil. *Eur J Pharm* **521**(1-3): 79-85.

Beedle AM, Hamid J, and Zamponi GW (2002). Inhibition of transiently expressed low- and high-voltage-activated calcium channels by trivalent metal cations. *J Mem Biol* **187:** 225–238.

Bender KJ, Uebele VN, Renger JJ, and Trussell LO (2012). Control of firing patterns through modulation of axon initial segment T-type calcium channels. *J Physiol* **590**: 109-118.

Blair NT and Bean BP (2002). Roles of tetrodotoxin (TTX)-sensitive Na^+ current, TTX-resistant Na^+ current, and Ca^{2+} current in the action potentials of nociceptive sensory neurons. *J Neurosci* ***22***(23): 10277–10290.

Bourinet E, Alloui A, Monteil A, Barrere C, Couette B, Poirot O, Pages A, McRory J, Snutch TP, Eschalier A, and Nargeot J (2005). Silencing of the Cav3.2 T-type calcium channel gene in sensory neurons demonstrates its major role in nociception. *EMBO J* **24**(2): 315-324.

Cain SM and Snutch TP. (2010). Contributions of T-type calcium channel isoforms to neuronal firing. *Channels (Austin)* **4**: 475-482.

Catterall WA, Dib-Hajj S, Meisler MH, and Pietrobon D (2008). Inherited neuronal ion channelopathies: new windows on complex neurological diseases. *J Neurosci* **28** (46): 11768–11777.

Catterall WA, Perez-Reyes E, Snutch TP, and Striessnig J (2005). International Union of Pharmacology. XLVIII. Nomenclature and structure-function relationships of voltage-gated calcium channels. *Pharmacol Rev* **57**(4): 411-25.

Choi S, Na HS, Kim J, Lee J, Lee S, Kim D, Park J, Chen CC, Campbell KP, and Shin HS (2007). Attenuated pain responses in mice lacking Ca(V)3.2 T-type channels. *Genes Brain Behav* **6**(5): 425-431.

Cregg R, Momin A, Rugiero F, Wood JN and Zhao J (2010). Pain channelopathies. *J Physiol* **588**(11): 1897–1904.

Cribbs L (2010). T-type calcium channel expression and function in the diseased heart. *Channels (Austin)* **4**(6): 447-452.

Cummins TR, Sheets PL, and Waxman SG (2007). The roles of sodium channels in nociception: implications for mechanisms of pain. *Pain* **131**:243–257.

David LS, Garcia E, Cain SM, Thau E, Tyson JR, and Snutch TP (2010). Splice-variant changes of the Ca(V)3.2 T-type calcium channel mediate voltage-dependent facilitation and associate with cardiac hypertrophy and development. *Channels (Austin)* **4**(5): 375-389.

Feng ZP, Doering CJ, Winkfein RJ, Beedle AM, Spafford JD, and Zamponi GW (2003). Determinants of inhibition of transiently expressed voltage-gated calcium channels by ω-conotoxins GVIA and MVIIA. *J Biol Chem* **278:** 20171–20178.

Heron SE, Khosravani H, Varela D, Bladen C, Williams TC, Newman MR, Ingrid E. Scheffer IE, Berkovic SF, Mulley JC, and Zamponi GW (2007). Extended spectrum of idiopathic generalized epilepsies associated with *CACNA1H* functional variants. *Ann Neurol* **62**: 560–568.

Hildebrand ME, Smith PL, Bladen C, Eduljeea C, Xie JY, Chen L, Fee-Maki M, Doering CJ, Mezeyova J, Zhu Y, Belardetti F, Pajouhesh H, Parker D, Arneric SP, Parmar M, Porreca F, Tringham E, Zamponi GW, and Snutch TP (2010). A novel slow-inactivation-specific ion channel modulator attenuates neuropathic pain. *Pain* **152** (4):833-843.

Hille, B (1977). Local anesthetics: hydrophilic and hydrophobic pathways for the drug-receptor reaction. *J Gen Physiol* **69**: 497–515.

Ikeda H, Heinke B, Ruscheweyh R, and Sandkuhler J (2003). Synaptic plasticity in spinal lamina I projection neurons that mediate hyperalgesia. *Science* **299**: 1237–1240.

Isom LL (2001). Sodium channel α subunits: Anything but auxiliary. *Neuroscientist* **7**: 42.

Jarecki BW, Piekarz AD, Jackson JO, and Cummins TR (2010). Human voltage-gated sodium channel mutations that cause inherited neuronal and muscle channelopathies increase resurgent sodium currents. *J Clin Invest* **120**(1): 369-378.

Jarvis MF, Honore P, Shieh CC, Chapman M, Joshi S, Zhang XF, Kort M, Carroll W, Marron B, Atkinson R, Thomas J, Liu D, Krambis M, Liu Y, McGaraughty S, Chu K, Roeloffs R, Zhong C, Mikusa JP, Hernandez G, Gauvin D, Wade C, Zhu C, Pai M, Scanio M, Shi L, Drizin I, Gregg R, Matulenko M, Hakeem A, Gross M, Johnson M, Marsh K, Wagoner PK, Sullivan JP, Faltynek CR, and Krafte DS (2007). A-803467, a potent and selective Nav1.8 sodium channel blocker, attenuates neuropathic and inflammatory pain in the rat. *Proc Natl Acad Sci USA* **104**: 8520–8525.

Khosravani H and Zamponi GW (2006). Voltage-gated calcium channels and idiopathic generalized epilepsies. *Physiol Rev* **86**: 941–966.

Lipkind GM and Fozzard HA (2005). Molecular modeling of local anesthetic drug binding to voltage-gated sodium channels. *Mol Pharmacol* **68**: 1611–1622.

McGaraughty S, Chu K, Faltynek CR. Scanio MJC, Kort ME, and Jarvis MF (2008). A Selective Nav1.8 sodium channel blocker, A-803467 [5-(4-Chlorophenyl-N-(3,5-dimethoxyphenyl)furan-2-carboxamide], attenuates spinal neuronal activity in neuropathic rats*. J Pharm Exp Ther* **324**: 1204–1211.

Park J and Luo ZD (2010). Calcium channel functions in pain processing. *Channels (Austin)* **4**(6): 510-517.

Perez-Reyes E (2003). Molecular physiology of low-voltage-activated T-type calcium channels. *Physiol Rev* **83**: 117–161.

Prescott SA and De Koninck Y (2002). Four cell types with distinctive membrane properties and morphologies in lamina I of the spinal dorsal horn of the adult rat. *J Physiol* **539**: 817–836.

Ragsdale DS, McPhee, Scheuer T and Catterall WA. (1994). Molecular determinants of state dependent block of Na channels by local anesthetics. *Science* **265**: 1725-1228.

Sheets PL, Heers C, Stoehr T, and Cummins TR (2008). Differential block of sensory neuronal voltage-gated sodium channels by lacosamide [(2R)-2-(acetylamino)-N-benzyl-3-methoxypropanamide], lidocaine, and carbamazepine. *J Pharm Exp Ther* **326**(1): 89-99.

Wang W, Gu J, Li YQ, and Tao YX (2011). Are voltage-gated sodium channels on the dorsal root ganglion involved in the development of neuropathic pain? *Molecular Pain* **7**: 16.

Waxman SG, Cummins TR, Dib-Hajj S, Fjell J, and Black JA (1999). Sodium channels, excitability of primary sensory neurons and the molecular basis of pain. *Muscle Nerve* **22**: 1177–1187.

Yarov-Yarovoy V, Brown J, Sharp EM, Clare JJ, Scheuer T, and Catterall WA (2001). Molecular determinants of voltage-dependent gating and binding of pore-blocking drugs in transmembrane segment IIIS6 of the Na channel α subunit. *J Biol Chem* **276**: 20–27.

Yarov-Yarovoy V, Jancy C. McPhee JC, Diane Idsvoog D, Caroline Pate C, Scheuer T, and Catterall WA (2002). Role of amino acid residues in transmembrane segments IS6 and IIS6 of the Na channel α subunit in voltage-dependent gating and drug block. *J Biol Chem* **277**: 35393–35401.

Yu FH and Catterall WA (2004). The VGL-chanome: a protein superfamily specialized for electrical signaling and ionic homeostasis. *Sci STKE* (253), re15.

Footnote:

This work was supported by operating grants to GWZ from the Canadian Institutes of Health Research. GWZ is a Canada Research Chair and an Alberta Innovates – Health Solutions (AI-HS) Scientist. CB holds a T. Chen Fong studentship and an AI-HS studentship award.

Molecular Pharmacology Fast Forward. Published on June 13, 2012 as DOI: 10.1124/mol.112.079715
This article has not been copyedited and formatted. The final version may differ from this version.

Figure legends:

Figure 1. Tonic block of voltage-gated calcium channels by A803467. A. Representative current trace recorded from Cav3.2 channels transiently expressed in tsA-201 cells before and after application of 5 μM A803467. Currents were elicited by stepping from a holding potential of -110 mV to a test potential of -30 mV. B. Representative time course of development of and recovery from A803467 block. C. Ensemble dose response curve for tonic Cav3.2 channel inhibition by A803467. The solid line is a fit via the Hill equation. D. IC50s for tonic A803467 block of rat HVA and human LVA calcium channels. Data were obtained by fitting dose-response curves for each channel subtype (n=6 per channel). Error bars reflect standard errors.

Figure 2. A,B, Current voltage relations recorded prior and after application of 5 μM A803467 to hCav3.1 (A) or hCav3.2 (B) channels. Data from multiple paired experiments are included in each figure. C,D, Steady State inactivation curves for hCav3.1 (C) and hCav3.2 (D) channels in the absence (Control) and presence of 5μM A803467. Note the negative shift in half inactivation potential in the presence of A803467. The data were fitted with the Boltzmann equation, half inactivation potentials obtained from the fits were as follows: hCav3.1: control -74 mV, drug -84 mV; hCav3.2: control -64 mV, drug -71 mV.

Figure 3. Summary of IC50s for A803467 block of Cav3 channel subtypes in a partial slow inactivated state. The inset shows the whole cell voltage command protocol used to induce slow inactivation (i.e., a test pulse P1, followed by a 10 s conditioning pulse to -70 mV, a brief hyperpolarization to remove fast inactivation, and a second test pulse P2 to determine the fraction of slow inactivated channels). Note that only Cav3.2 channels display a decrease in

IC50 for A803467 inhibition during P2, indicating a selective increase of A803467 affinity for slow inactivated Cav.3.2 channels (*p < 0.05, Student's T-test).

Figure 4. Sequence alignment of the local anesthetic binding regions in Nav channels with the analogous regions in hCav3.2. Residues involved in local anesthetic binding to Nav channels are indicated in bold. Note the overall degree of sequence similarity between T-type channels, sodium channels and the NavAb bacterial sodium channel whose crystal structure has recently been resolved.

Figure 5. Summary of IC50s for tonic A803467 block of wild type (Wt) and mutant Cav3.2 channels. Currents were elicited by stepping to a test potential of -30 mV from a holding potential of -110 mV. Significance was assessed using ANOVA (**p < 0.01)

Figure 6. IC50 values for A803467 block of slow inactivated Cav3.2 channels using the same protocol as that described in Figure 3 except holding potential was stepped to -80 mV. Note that the mutant channels do not show an increase in blocking affinity for the slow inactivated state (*p < 0.05, t-test).

Figure 7. Effect of a tyrosine substitution in position 1855 of hCav3.2. A. IC50 for tonic A803467 of Wt and mutant V1855Y (*p < 0.05, t-test). B. Steady state inactivation curves recorded in the presence and the absence of 5 μM A803467. Note the hyperpolarizing shift from -58 mV to -64 mV. For comparison, the inactivation curve of the Wt (Control) channel is included. C. Dose dependence of slow inactivated channel block of mutant hCav3.2 V1855Y

Molecular Pharmacology Fast Forward. Published on June 13, 2012 as DOI: 10.1124/mol.112.079715
This article has not been copyedited and formatted. The final version may differ from this version.

expressed as the fractional current at various drug concentrations. The inset depicts the IC50 for P1 vs P2 slow inactivated channel block by A803467 using same protocol as described in Figure 3. Note that the Tyrosine substitution produces submicromolar block by this compound.

Figure 8. Summary of IC50s for tonic A803467 block of wild type (Wt) and mutant Q1848L and Q1848F hCav3.2 channels. Currents were elicited by stepping to a test potential of -20 mV from a holding potential of -110 mV. Asterisks denote statistical significance relative to control (**$p<0.01$). All recordings in this figure were performed in 20 mM Barium due to the small current amplitudes of the mutants. IC50 values were obtained by fitting dose response curves with the Hill equation as described in Figure 1. Both substitutions in position 1848 produced submicromolar block by this compound.

Molecular Pharmacology Fast Forward. Published on June 13, 2012 as DOI: 10.1124/mol.112.079715
This article has not been copyedited and formatted. The final version may differ from this version.

Table 1.

Calcium Channel	$V_{0.5}$act (mV) Con	$V_{0.5}$act (mV) Drug	V*h* (mV) Con	V*h* (mV) Drug	IC50 Tonic (μM)
hCav3.1	-50.3 ±1.6 N=5	-60.0 ±1.6* N=5	-74 ±0.9 N=5	-84 ±1.8* N=5	4.8 N=6
hCav3.2	-44.3 ±1.4 N=7	-52.1 ±1.2* N=7	-64.2 ±0.93 N=5	-71 ±0.45** N=5	7.0 ±0.51 N=6
hCav3.3	-47.8 ±1.6 N=6	-50.0 ±2.7 N.S. N=6	-79 ±1.7 N=9	-83 ±1.6 N.S. N=9	5.6 N=6
rCav2.1	-15.8 ±1.3 N=5	-25 ±1.4 N=5	N.A.	N.A.	15.0 N=6
rCav1.2					50.0 N=6

Biophysical parameters of HVA and LVA calcium channels in the absence and the presence of A803467. Asterisks denote statistical significance relative to control (*p<0.05, **p<0.01, N.S. – not significant).

Molecular Pharmacology Fast Forward. Published on June 13, 2012 as DOI: 10.1124/mol.112.079715
This article has not been copyedited and formatted. The final version may differ from this version.

Table 2.

Calcium Channel	$V_{0.5}$act (mV)	E_{rev} (mV)	Gmax (μS)	V*h* (mV)	IC50 Tonic (μM)
hCav3.2	-44.3 ± 1.4 N=7	27.3 ± 0.7 N=7	-1.9 ± 0.08 N.S N=7	-64.2 ± 0.93 N.S. N=5	7.0 ± 0.51 N=6
hCav3.2 I403A	-54.0 ± 1.8* N=11	20.3 ± 1.8* N=11	-1.7 ± 0.09 N.S N=11	-63.8 ± 0.87 N.S. N=6	20.0 ± 1.5 ** N=6
hCav3.2 V1551A	-47.0 ± 1.1 N.S. N=13	23.8 ± 1.5 N.S. N=13	-1.9 ± 0.06 N.S N=13	-67.0 ± 0.98 N.S. N=6	40.0 ± 3.1** N=6
hCav3.2 V1855Y	-29.64 ± 2.1* N=14	14.64 ± 2.1* N=14	-3.9 ± 0.14* N=14	-58.4 ± 0.56* N=6	1.8 ± 0.41* N=6

Biophysical parameters of wild type and mutant hCav3.2 calcium channels. Asterisks denote statistical significance relative to wild type (*$p<0.05$, **$p<0.01$, N.S. – not significant).

Figure 1.

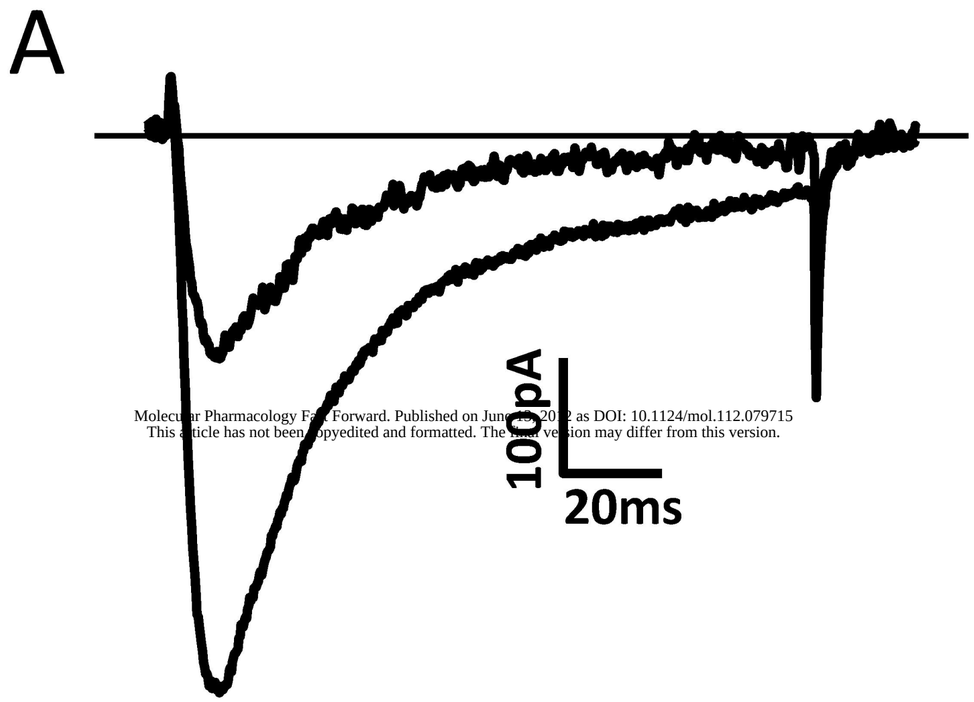

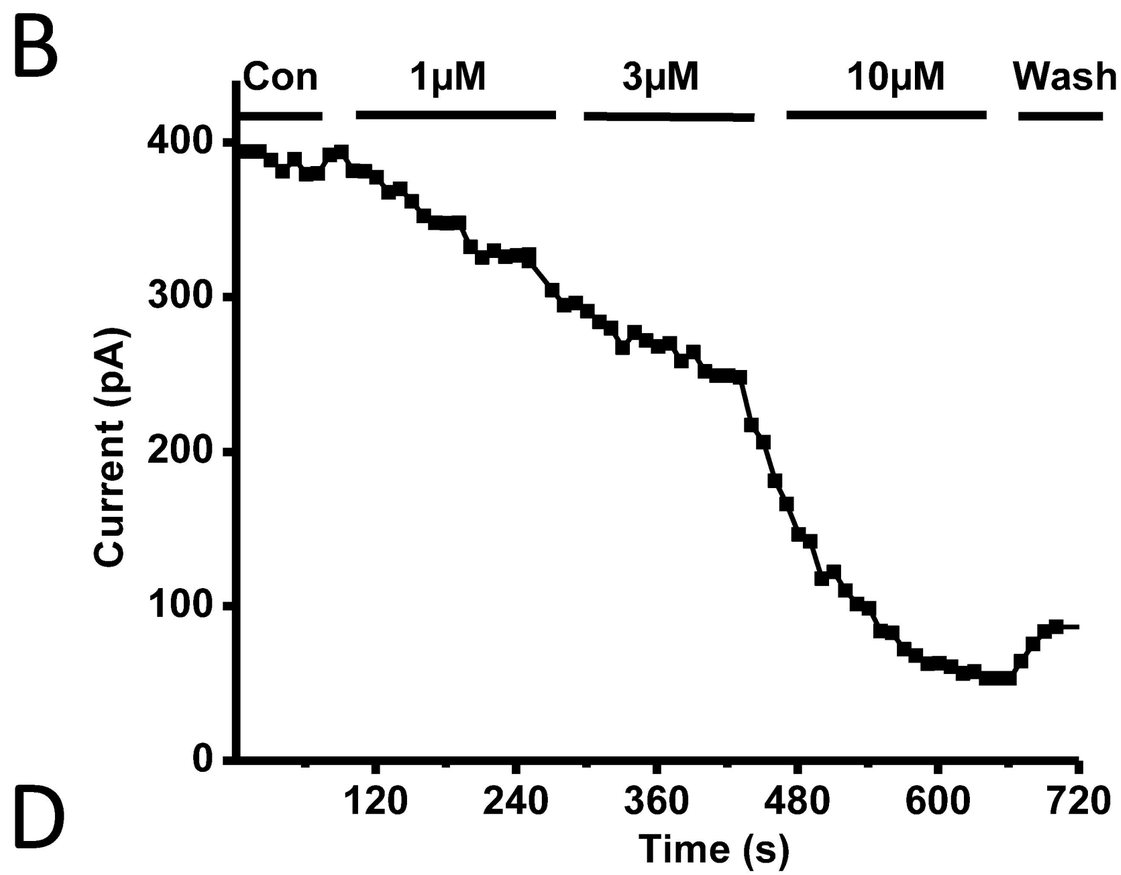

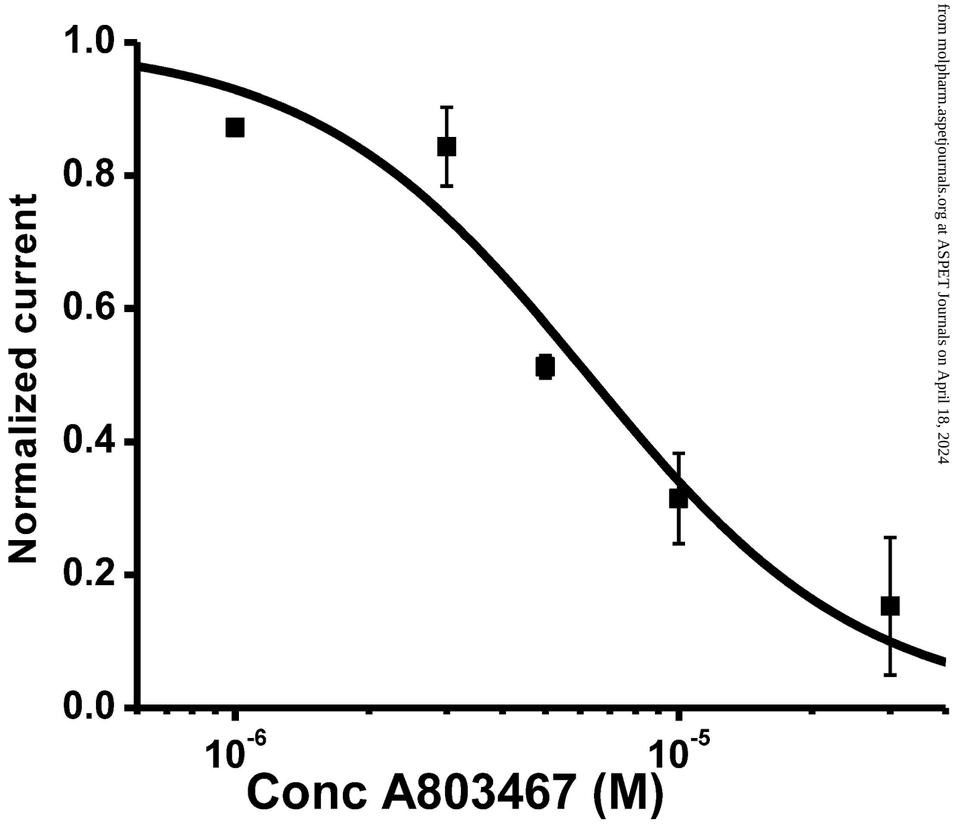

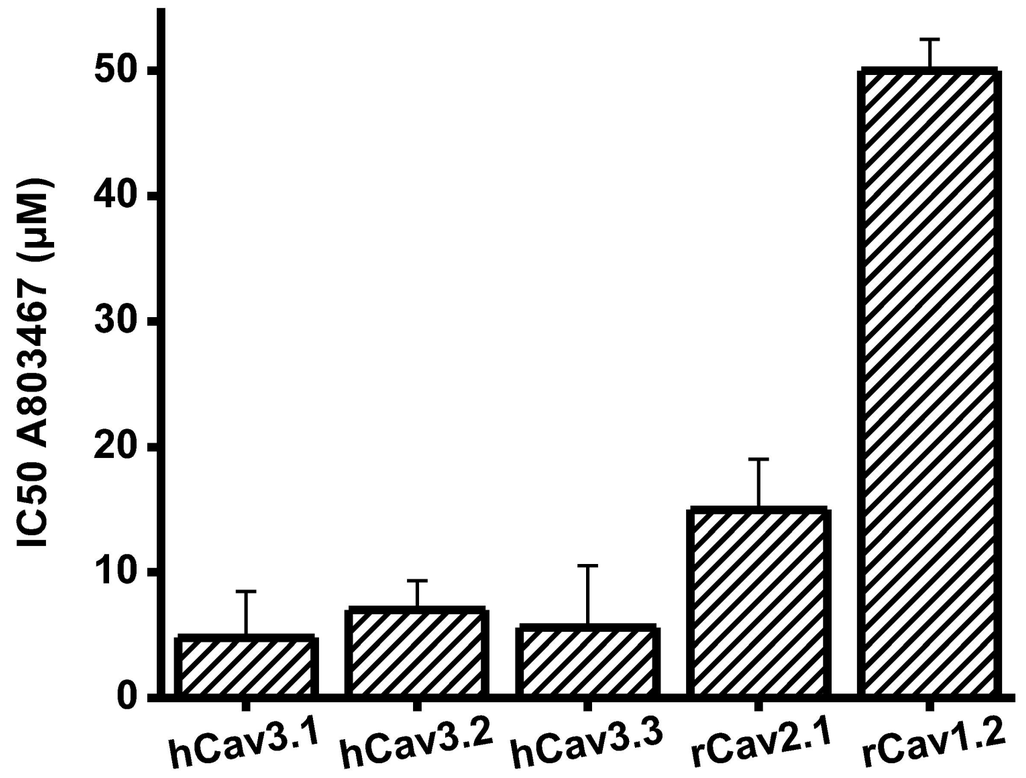

Figure 2.

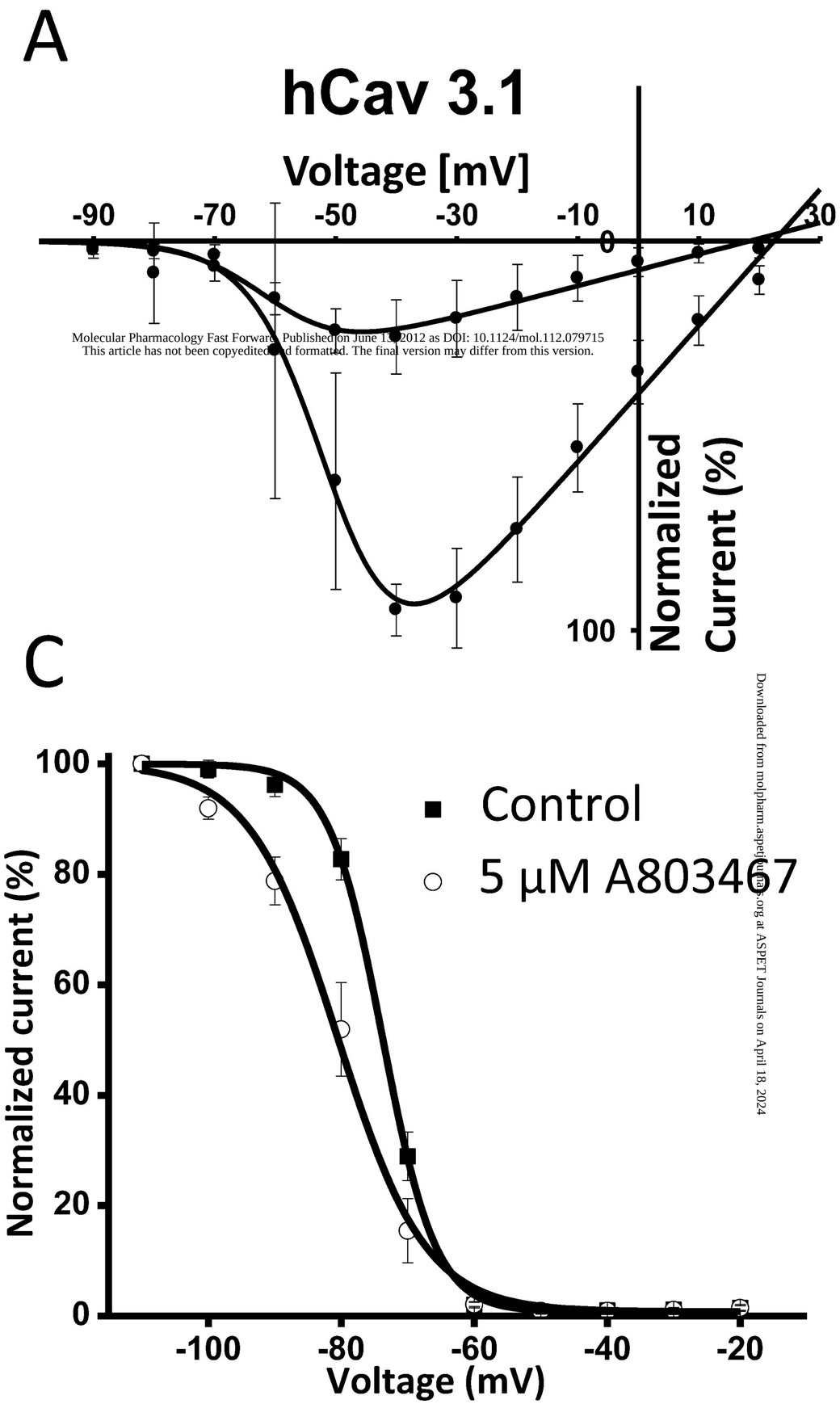

Figure 3.

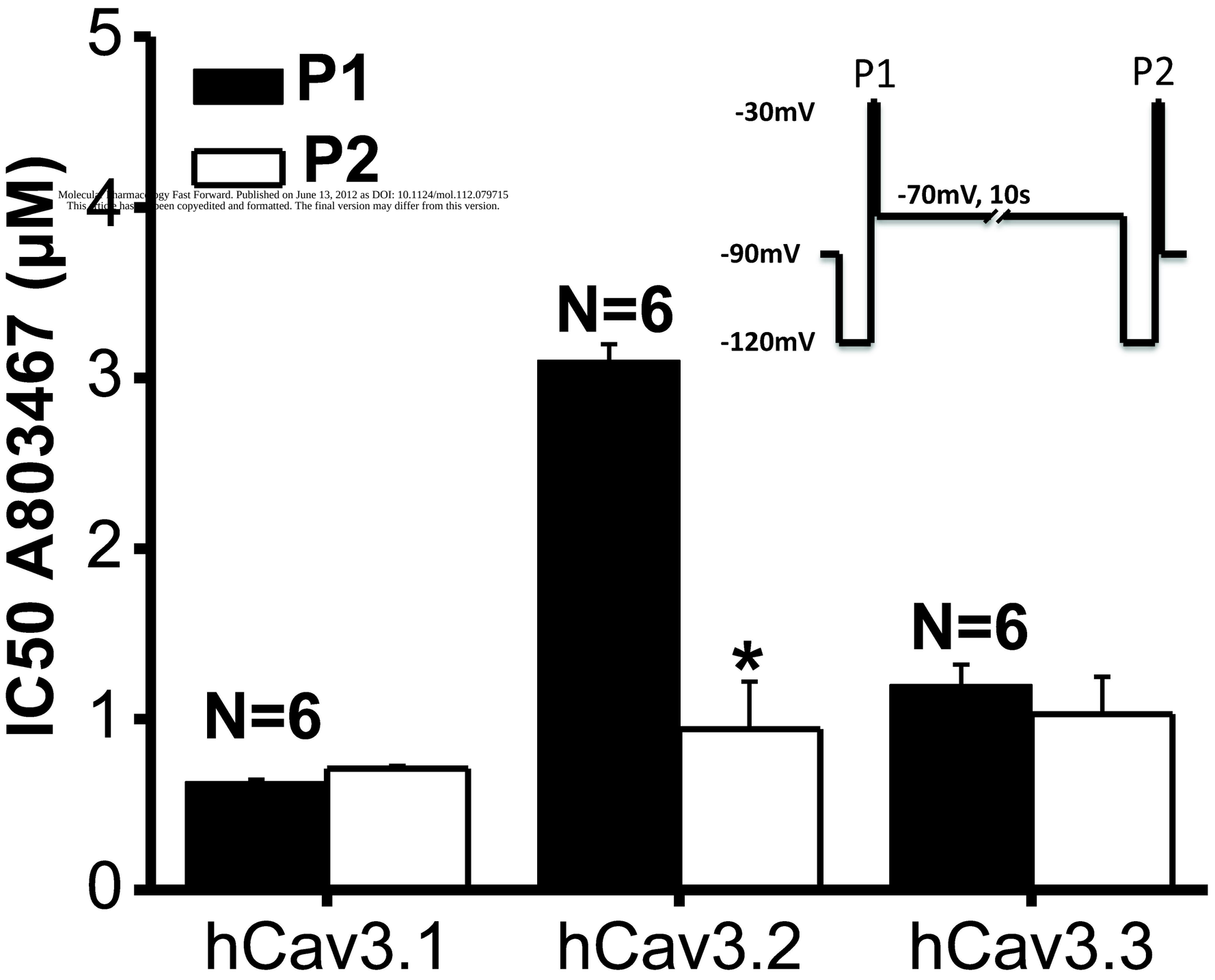

Figure 4.

```
Nav1.8    YMIFFVLVIFLGSFYLVNLILAVVT 397
Nav1.2    YMIFFVLVIFLGSFYLINLILAVVA 425
Cav3.2    NFIYFILLIIVGSFFMINLCLVVIA 419
             .*.:*.*:*::*********** *.*::

              :::*: **:.  *. :**.*.:*:*
NavAb     AWVFFIPFIFVVTFVMINLVVAIIVD-- 219
Nav1.8    MYLYFVIFIIFGGFFTLNLFVGVIIDNF 1421
Nav1.2    MYLYFVIFIIFGSFFTLNLFIGVIIDNF 1476
Cav3.2    MLLYFISFLLIVSFFVLNMFVGVVVENF 1558
          * ***: *::: .**.**:*:**::**

Nav1.8    PAVGIIFFTTYIIISFLIMVNMYIAV 1720
Nav1.2    PSVGIFFFVSYIIISFLVVVNMYIAV 1774
Cav3.2    PALSPVYFVTFVLVAQFVLVNVVVAV 1858
          *:. .:*.:::::: :::**: :**
```

Figure 5.

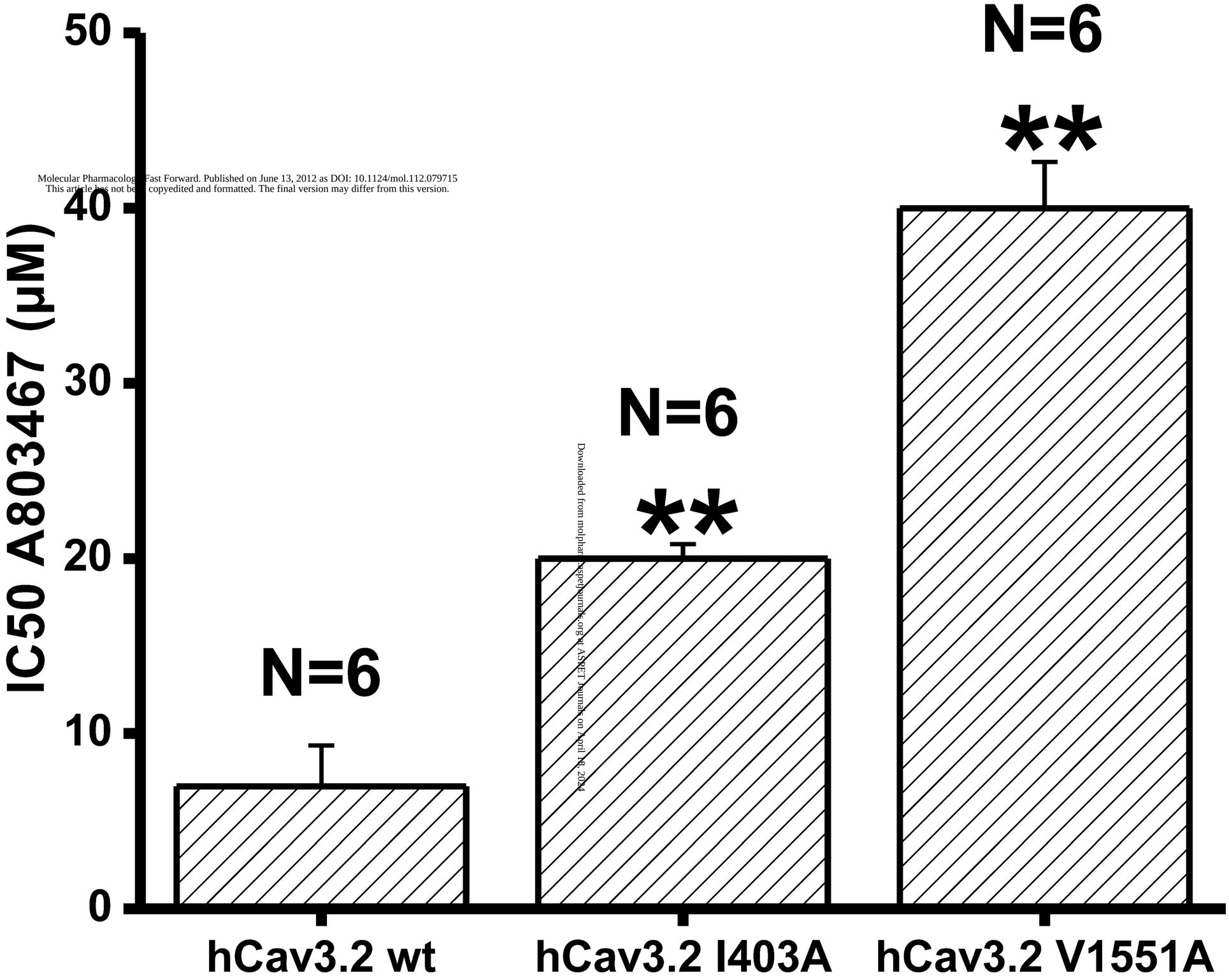

Figure 6.

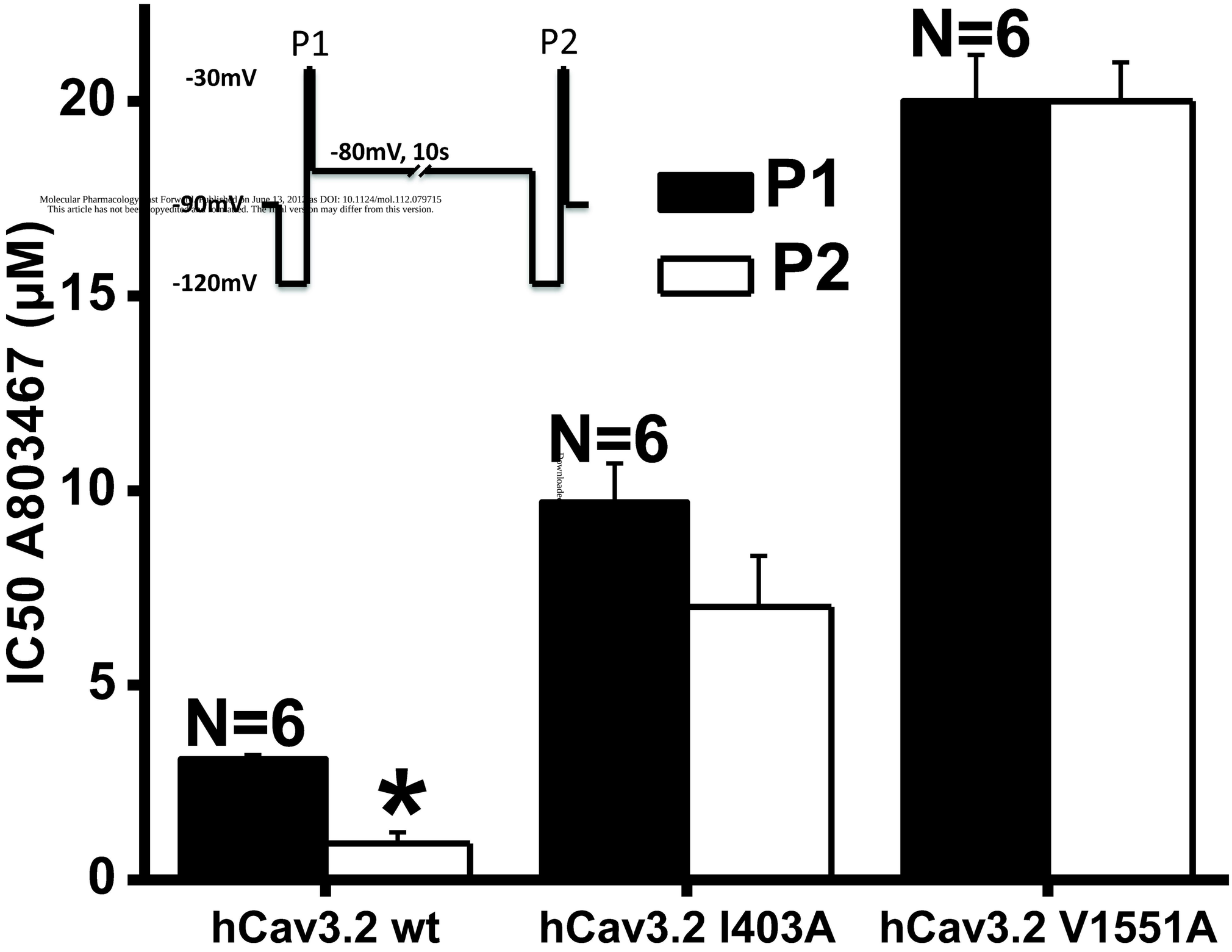

Figure 7.

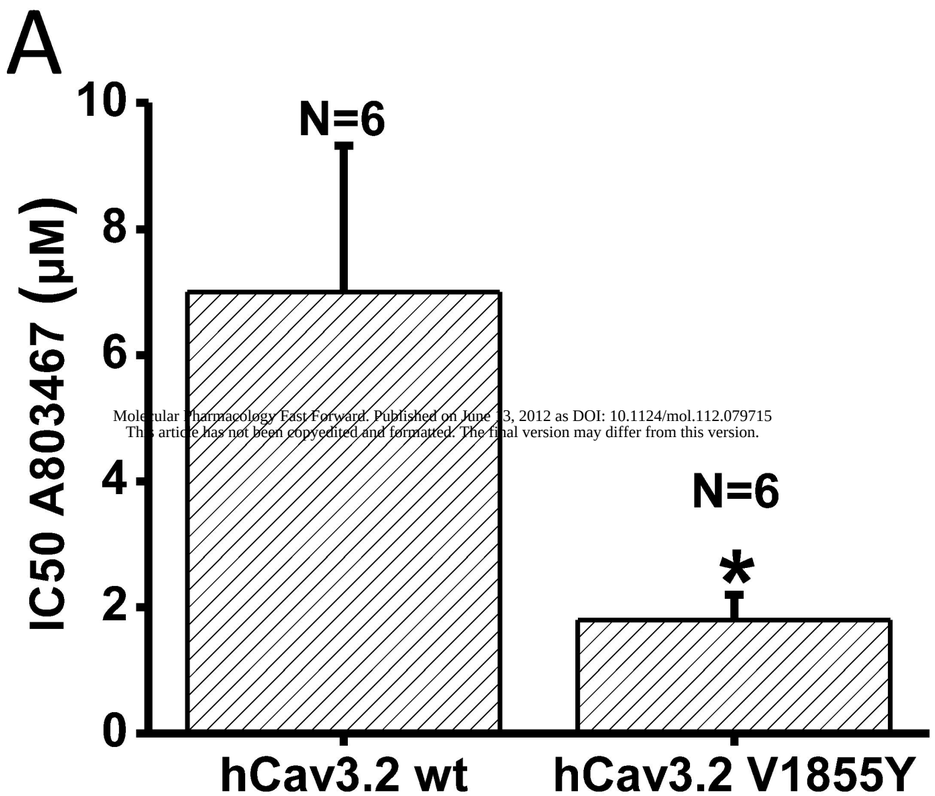

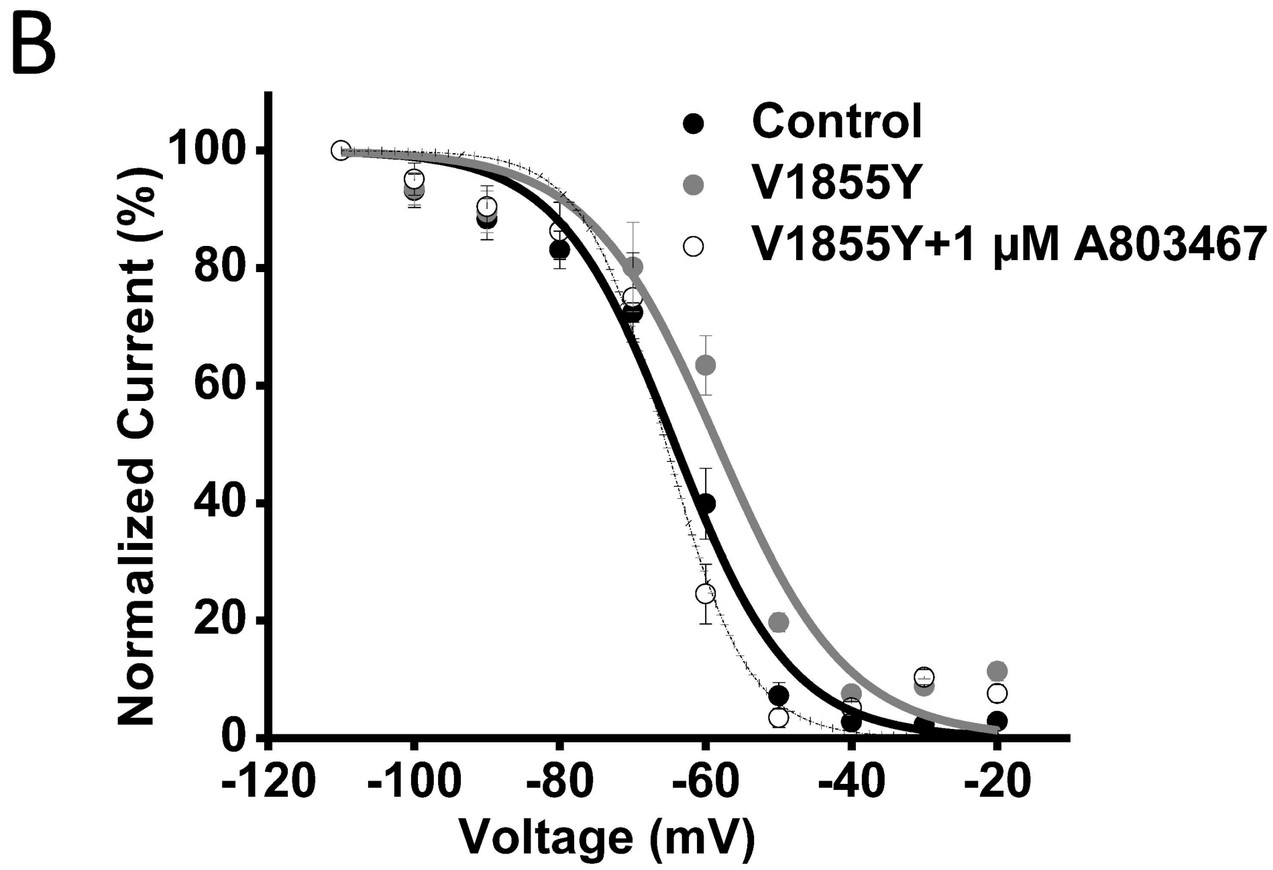

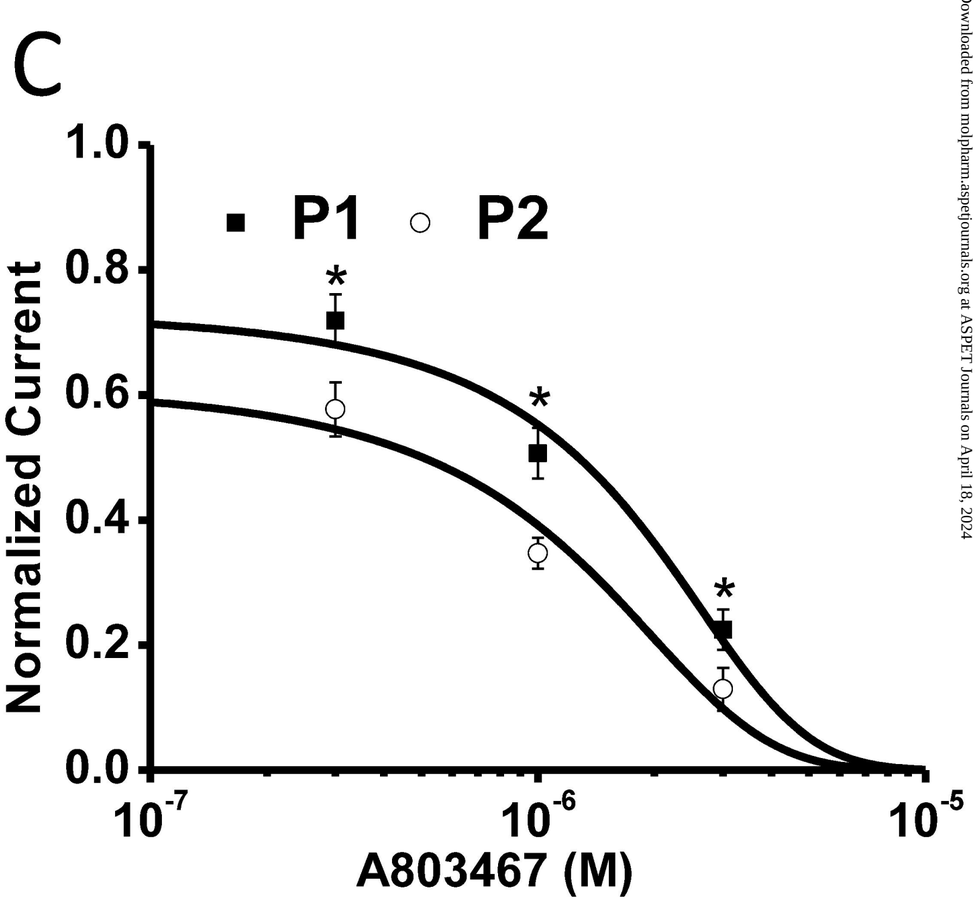

Figure 8.